Psychological Research (2022) 86:1683–1697
https://doi.org/10.1007/s00426-021-01589-0

ORIGINAL ARTICLE

The Z-Box illusion: dominance of motion perception among multiple 3D objects

Joshua E. Zosky[1] · **Michael D. Dodd**[1]

Received: 20 April 2021 / Accepted: 27 August 2021 / Published online: 4 September 2021

Abstract
In the present article, we examine a novel illusion of motion—the Z-Box illusion—in which the presence of a bounding object influences the perception of motion of an ambiguous stimulus that appears within. Specifically, the stimuli are a structure-from-motion (SFM) particle orb and a wireframe cube. The orb could be perceived as rotating clockwise or counterclockwise while the cube could only be perceived as moving in one direction. Both stimuli were presented on a two-dimensional (2D) display with inferred three-dimensional (3D) properties. In a single experiment, we examine motion perception of a particle orb, both in isolation and when it appears within a rotating cube. Participants indicated the orb's direction of motion and whether the direction changed at any point during the trial. Accuracy was the critical measure while motion direction, the number of particles in the orb and presence of the wireframe cube were all manipulated. The results suggest that participants could perceive the orb's true rotation in the absence of the cube so long as it was made up of at least ten particles. The presence of the cube dominated perception as participants consistently perceived congruent motion of the orb and cube, even when they moved in objectively different directions. These findings are considered as they relate to prior research on motion perception, computational modelling of motion perception, structure from motion and 3D object perception.

Introduction

The human visual system converts input from the environment into a rich perceptual experience through a variety of co-occurring processes. Given the complexity of our visual world, however, it can be difficult to examine individual perceptual processes in isolation. The study of optical illusions is one way of overcoming this complexity. Many optical illusions constitute errors of perception—one percept is expected but another is observed—which inform us of the subtle mechanisms generating perceptual experience. The present paper introduces a novel visual illusion—the Z-Box Illusion—which has ramifications for studying perceptual stability and motion in multiple objects.

As is often the case with illusions, the Z-Box Illusion was an accidental discovery. The illusion was first observed while generating displays for a graphics demo. The demo's display consisted of a particle-orb and wireframe cube, each spinning on the *y* axis in opposite directions (incongruent motion, as demonstrated in Online Resource 1). Surprisingly, observers reported that both objects moved in the same direction (congruent motion). The observers' perception of congruent motion persisted, despite being informed of the incongruent motion hard-coded into the demo (from here on the programmed direction of motion will be referred to as the "Coded Direction," to distinguish it from the viewer's perception which will be referred to as the "Perceived Direction"). Further, any attempts to override the erroneous percept required significant effort. The illusion was subsequently named the "Z-Box Illusion," referring to the depth plane—in a Cartesian coordinate system—and wireframe cube which drew attention to the perceptual anomaly. Demonstrations of the illusion in multiple variations—both informally with colleagues (i.e. graduate students, post-docs, professors and lab members) and formally at the Vision Sciences Society's 2017 Demo-Night—led to a consensus amongst observers. In viewing the orb alone, it was perceived as a bistable (ambiguous) object which could rotate in either clockwise or counterclockwise direction (when imagined from a bird's-eye view). Although some viewers could determine the orb's Coded Direction, all viewers commented that the orb's direction could be flipped between rotating clockwise or counterclockwise. When viewing the orb and

✉ Joshua E. Zosky
joshua.e.zosky@gmail.com

[1] Department of Psychology, University of Nebraska-Lincoln, Lincoln, NE, USA

cube together, the orb would stabilize (become unambiguous) and then revert to being bistable when the cube disappeared. Furthermore, the cube was decidedly a stable object with discernable front and back faces, and its 3D structure was not defined by motion (in contrast to the orb). Observers agreed that the orb's rotation was strongly influenced by the direction of the cube, and the orb's Perceived Direction would change any time the cube's direction changed. Finally, sparse numbers of particles constructing the orb led to perceptions of independently floating particles as opposed to a 3D orb. In contrast, higher particle counts increasingly interfered with the illusion of congruent motion between the orb and cube. These presentations provided valuable insight into the common perceptual experiences generating the illusion. The preliminary findings aided in linking prior research to the orb, the cube, and their interaction.

Characteristics of the orb

Despite the strong perception of a 3D orb, the orb is not a true 3D shape. This perception arises from a 2D display of individual particles whose trajectories are consistent with that of an orb's surface. All of the particles are projected onto a 3D space after calculating their random *X*, *Y* and *Z* coordinates relative to a shared central point and constant radius. Consistent with depth perception cues relative to the particles' central point, the particles drawn closer to the viewer travel faster and with nonparallel horizontal trajectories (i.e. an arc-shaped trajectory) relative to particles drawn distant from the viewer. Collectively, these properties should lead to the inferred perception of a 3D rotating orb. In contrast to the aforementioned depth cues, the particles were drawn with a constant size regardless of simulated distance from the viewer (i.e. particles closer to the viewer were the same size as relatively distant particles). The lack of this depth cue complicates inferences of a 3D orb, as the particles' size changes in depth should disambiguate the front-facing side versus back-facing side of the orb (i.e. particles closer to the viewer should be larger than particles distant from the viewer). This aspect of the orb seems related to the consensus that—while the motion of the particles creates an inference of a 3D orb—the perception of the orb's sides (front versus back) as well as rotational direction appear to be interchangeable. The properties of the orb relate to various fields of research while no single previous finding could account for all aspects of the orb's percept.

During pilot examinations of the illusion, the speed of rotation, axis of rotation, angle of rotation, and number of particles constituting the orb were all manipulated. The only property consistently influencing viewers' perception was the number of particles constructing the orb, wherein the perception of a 3D orb gained strength rapidly with increasing particle counts. Moreover, the orb appears to be related to studies examining structure from motion, support ratios, and 3D structure perception. Structure-from-motion (SFM) displays (Andersen & Bradley, 1998; Nawrot & Blake, 1989; Ramachandran et al., 1988; Treue et al., 1991) occur when 2D stimuli move relative to a common axis, subsequently grouping to form a perceptually unified 3D shape. SFM stimuli are frequently observed as bistable (ambiguous) with regards to their front and back faces (Miles, 1931; Wallach & O'Connell, 1953). In typical SFM studies, the 2D stimuli move in parallel trajectories about their common axis. Although the present illusion was presented with nonparallel particle trajectories, the orb shape still exhibited the bistable percept common to typical SFM stimuli. With regard to the number of particles presented, the orb seems related to the role of support ratios on illusory contours (Erlikhman et al., 2018, 2019; Shipley & Kellman, 1992). Support ratios are represented by the relationship of visible-to-illusory details defining a perceived shape. The perception is more ambiguous for ratios approaching 0:1 and less ambiguous for ratios approaching 1:1. In this regard, ambiguity in the 3D orb's perception should decrease as the number of particles increases. Previous studies have also suggested that 3D structures arise from motion ambiguity due to the stimuli's rigidity (i.e. structural integrity) and its smoothness of motion (Erlikhman et al., 2018, 2019; Hoffman & Bennett, 1986; Jain & Zaidi, 2011; Ullman, 1979, 1984). The orb's perceptual rigidity and smoothness are likely due to the Gestalt principle of common fate (Köhler, 1970), which proposes that when objects appear to move together, they are perceived as belonging together, also known as binding. The combination of these observations suggests that perception of the orb increases with more particles.

Characteristics of the cube

The wireframe cube is also a 3D shape inferred from a 2D display. In contrast to the orb, this percept relies less on motion cues due to the visible edges forming the outline of a cube shape. Each line was drawn after calculating the *X*, *Y* and *Z* coordinates for its endpoints in 3D space relative to a shared central point and constant distance from said point. When rotating, the cube's edges appeared to grow and shrink according to the rules of motion parallax (lines appear larger the closer they are to the viewer; Rogers & Graham, 1979). Unlike the orb, the cube was considered a stable object with a consistently discernable front versus back face. Although frequently as compared to a Necker cube (Bradley & Petry, 1977), the Z-Box's faces were typically incapable of being perceptually flipped from front-face to back face. This was likely due to the differently sized edges dependent upon where they lie in the *Z* plane. As a result, observers considered the orb a structurally weaker stimulus than the cube.

The interaction of the orb and cube

The simultaneous presentation of the orb and cube—and the subsequent illusion— further relates to studies of both the motion aperture problem and feature-based attention. As highlighted by the barber pole illusion (Wuerger et al., 1996), the motion aperture problem is an inability to infer the objective direction of motion for an object due to limited visual input (i.e. small aperture). Increasing visual input—a larger aperture—resolves the ambiguity. Without the added context from a larger aperture, an object's direction of motion binds to prior expectations or nearby stimuli. In the Z-Box illusion, the orb's Perceived Direction is ambiguous due to limited perceptual information. The movement of the box surrounding the orb adds contextual details (i.e. increases the aperture). This increase in aperture decreases the ambiguous perception of the orb's Perceived Direction. Similarly, research in feature-based attention has shown that task-irrelevant stimuli (i.e. the cube) can bias depth perception for task-relevant stimuli (i.e. the orb's front versus back face; Yu et al., 2017). This suggests the cube is capable of forcing the orb's Perceived Direction by flipping front and back faces.

Related work in the computational modelling of motion disambiguation lends further support to the orb's susceptibility to perceptual error. In particular, Weiss and Adelson (1998) proposed a Bayesian computational model for motion perception that could explain a variety of motion illusions when biasing the model towards slow and smooth motion. In a follow up report, they found that a motion perception model biased for smoothness of motion (i.e. the change in distance and location of particles with each display update) best explained ambiguous motion perception for a rotating 2D ellipse (Weiss & Adelson, 2000). Their work later showed that their model with bias for slower motion outperformed unbiased models when examining the motion aperture problem (Weiss et al., 2002). Taken together, these findings suggest that the orb's smoothness of motion and rotational speed relate to the strength of perceived motion at a computational level. Similar to models of slow and smooth motion, Domini and Caudek (Caudek & Domini, 1998; Domini & Caudek, 2003) repeatedly demonstrate that depth perception cannot be reconciled by stimulus properties alone. The authors conclude that a heuristic model—in which physical properties of the stimulus, viewing conditions of the observer and accounting for noise in perceptual judgements (also referred to as observer measurement uncertainty; Domini & Caudek, 2010)—best approximate results in human perception. This theory suggests that visual properties of the stimuli are insufficient for generating stable motion perception. Disentangling the independent rotation direction for the orb and cube relies on observers' perceptual uncertainty meaning that a stimulus' perceptual stability (e.g. the number of particles constructing the orb) may be a critical aspect to observers' perceptual uncertainty. These initial observations along with insight from related findings were used to inform the design of the present study.

The present study

Given the perceptual experiences reported above, the present study sought to assess the strength of this novel illusion and to determine the critical features driving its illusory percept. We sought to answer the following questions: is the orb's Coded Direction perceivable? If so, is the orb's Coded Direction still perceivable when presented with the cube? To test these questions, a two-phase experiment was designed to first examine perception of the orb on its own, then subsequently examine the influence of the cube on perception of the orb.

In Phase 1, a 3D particle-orb was presented—with a range of particle counts—to test participants' ability to accurately perceive the orb's Coded Direction. In Phase 2, three types of trials were presented to participants: (1) An orb alone trial—identical to Phase 1 trials—to test participants' ability to perceive the orb's Coded Direction when intermixed with cube presentations; (2) An orb and cube trial where each object rotated in a single direction for the entire trial (with congruous or incongruous motion between the objects). This tested participants' ability to perceive the orb's Coded Direction when presented with the cube and their susceptibility to perceive the orb spinning the same direction as the cube. (3) An orb and cube trial, identical to the one just mentioned, with the inclusion of the cube flipping direction after participants' initial response to determine whether they subsequently updated their response. These trials further test participants' susceptibility to the illusion even after the cube changes direction. Finally, all trials presented the orb as either 1, 10, 100 or 1000 particles to assess the influence of particle count on response accuracy.

Based on the literature and feedback from presentations, it was expected that the orb's Coded Direction would be identifiable without the cube, regardless of Phase 1 or Phase 2 designs. Furthermore, the inclusion of the cube in Phase 2 would make the orb's direction ambiguous as it would be perceived as moving the same direction as the cube even if that direction changes. Finally, increases in the orb's particle count would contribute to increased accuracy when the orb is presented alone, but it will not impact trials with the cube present.

Experiment

There were two phases to the present experiment. Phase 1 was a baseline test of participants' ability to determine the direction of motion for a 3D particle orb of varying

complexity (measured by number of particles). Phase 2 was a follow-up test of the same task and stimuli with the inclusion of a 3D wireframe cube (for examples of Phase 1 and Phase 2 trials, see demonstration in Online Resource 1). The experiment presented different combinations of particles per orb, direction of orb and direction of the cube to determine the influence of these factors on motion perception.

A pilot study was conducted prior to the current study. The current study matched the pilot study methodologically with the addition of orb alone trials in phase 2. A statistical power analysis was performed using *G**Power 3.1 (Faul et al., 2007) for sample size estimation based on data from the pilot study ($N = 36$). The power analysis specifically focused on the ANOVA analysis of response accuracy for the main effect of particle count and the main effect of motion congruency of the orb and cube. Effect sizes ranged from 0.37 (Cohen's *f*; for the main effect of particle count) to 2.71 (Cohen's *f*; for the main effect of orb and cube congruency). We focused on the smaller effect of particle count as this would require a larger sample size for replication. With an alpha = 0.05 and power = 0.95, the projected sample size needed with this effect size is approximately $N = 26$ for the simplest within group comparison. To account for an additional condition in Phase 2 and allow for experimental issues such as attrition, our proposed sample size of N = 40 was determined to be more than adequate.

Methods

Participants

Forty-one undergraduate students from the University of Nebraska–Lincoln participated in a single experimental session and received course credit for their participation. All participants had normal or corrected-to-normal vision and were naïve to the purpose of the experiment which took approximately 30 min. Anyone previously exposed to the illusion was excluded from participation in the study. Owing to a scheduling error, an extra participant was recruited in the study beyond the proposed sample size of forty.

Materials

All stimuli are presented in Fig. 1. Experiment and stimulus design occurred in Vizard 5 (WorldViz, Inc.), a Python programming IDE designed for 3D and virtual reality development. Vizard uses metric measurements within 3D renderings for accurate portrayals of distance in virtual space. The central point for all experimental stimuli was located at 0 on the *X* and *Y* axes and a distance of 5 m from the viewpoint on the *Z* axes. Within the 3D space, no shading effects were enabled and the background was grey (the median of black and white values). Antialiasing was utilized in all stimuli to simulate smooth motion, which led to minor color blending (1 pixel could generate 0–8 adjacent pixels of blended colors). Blending was determined to increase drawings (points and lines) by a maximum of 0.1° of visual angle per pixel. A Dell U2312HM Flat Panel Monitor (Dell, Inc.) was used for stimulus presentation with a refresh rate of 60 Hz, screen resolution of 1920 × 1080 and display size of 509.2 mm × 286.4 mm.

Stimuli

Example videos of all stimuli can be found in Online Resource 1. The stimuli consisted of an orb shape and

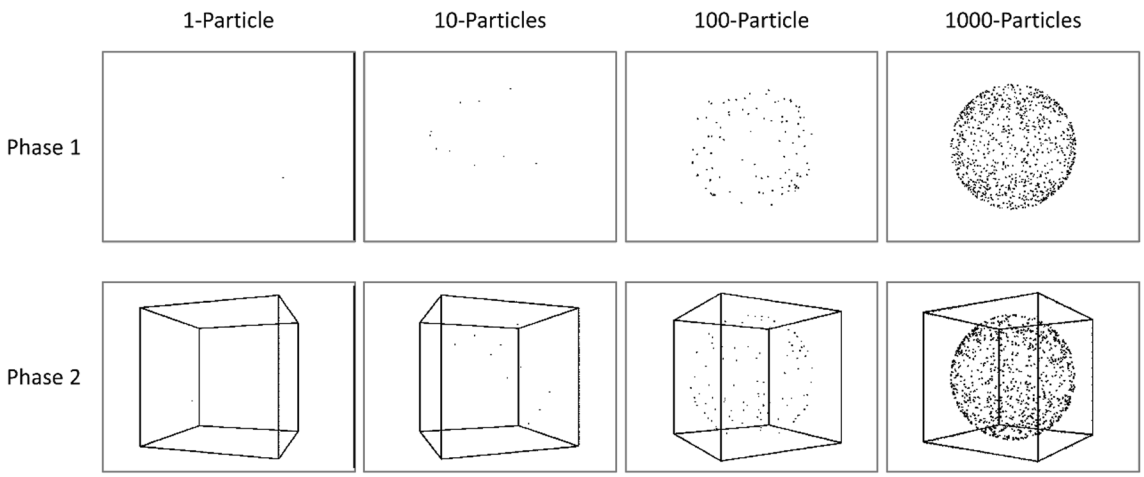

Fig. 1 Stimuli used in the experiment. The top row shows stimuli found in Phase 1 where the orb is alone. The bottom row shows stimuli from Phase 2 with the cube and orb. The actual displays consisted of a grey background, white cube and black particles, but are presented here in black and white for clarity

cube shape. The orb's diameter measured approximately 9.85° visual angle. The cube's width and height—when oriented 90° (i.e. front face square towards viewer)—was measured to be approximately 11.81° visual angle. When oriented 45° (i.e. side-edge centered towards viewer)—the cube was measured to be approximately 13.36° visual angle in width and approximately 13.21° visual angle in height.

The orb shape is inferred by the motion of surface-based particles rotating about the *Y*-axis. Each particle was set to 2 pixels^2 in size—regardless of distance from the viewpoint—and black in color. With shading from anti-aliasing, this altered the particle's size from 2 pixels^2 to 4 pixels^2 or from 0.05° to 0.10° of visual angle. The orb was constructed of either 1, 10, 100 or 1000 particles on each trial. Within the metric scale of the 3D environment, each particle was randomly assigned a location 0.5 m away from the central point, resulting in a diameter of 1 m (as measured within the 3D environment's standard units). The only constraint on particle location occurred for single-particle trials which were only allowed vertically between −45° and +45° from the orb's zero *Y* coordinate. This was to avoid trials where the particle had limited trajectory across the screen (e.g. making small rotations near the top or bottom poles of the orb) and could lead to edge-case scenarios.

The cube is a 1 m^3 wireframe consisting of 2 pixel-thick—regardless of distance from the viewpoint—white lines. The colors were selected to create striking contrast between the stimuli to ensure no ambiguous overlap between the stimuli. Both objects rotated at an absolute speed of 45° per second. Rotation direction was defined relative to the orb's front-face. Left-spin was defined by clockwise rotation around the *Y* axis and counterclockwise rotation was right-spin (as observed from a bird's-eye view, see Fig. 2). To preface the results, there was no influence of orb rotation direction, only congruence/incongruence with the cube. As such, the data were collapsed across this variable. Congruent motion is defined as both orb and cube rotating the same direction, while incongruent motion is defined as the orb rotating the opposite direction of the cube.

To simplify discussion, letters and symbols will be used to represent the conditions in Phase 1 and Phase 2 (see Table 1 for complete breakdown and Fig. 2 for visual breakdown). The only manipulation common to both Phase 1 and Phase 2 was particle count (**1/10/100/1000**). The manipulations exclusive to Phase 2 are cube presence [**O**rb **a**lone (**Oa**)/**O**rb and **c**ube (**Oc**)] and motion congruency (**C**ongruent motion/**I**ncongruent motion). For example, a clockwise spinning 10 particle orb and a motion incongruent counterclockwise spinning cube trial can be represented as **10OcI**.

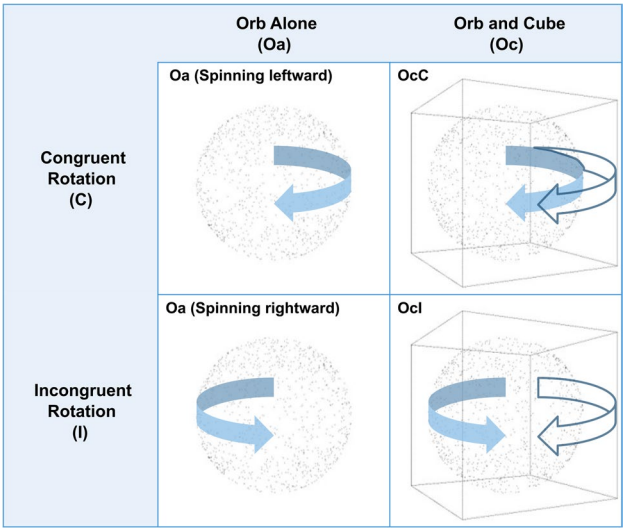

Fig. 2 Conditions presented within the experiment. Columns present the Orb Alone trials (**Oa**) and the Orb and Cube trials (**Oc**). The top row shows stimuli rotating the same direction around the orb's Y axis, or Congruent Rotation (**C**), while the bottom row shows stimuli rotating opposite directions, or Incongruent Rotation (**I**). Shaded arrows represent the orb's Coded Direction and outlined arrows represent the cube's rotation direction (when seen from bird's eye view). The actual displays consisted of a grey background, white cube and black particles

Procedure

Participants were seated approximately 60 cm from the computer monitor with a keyboard for response collection. The experiment consisted of a brief onscreen training and two task phases.

Video of the instruction screen for Phase one can be seen at Online Resource 2. First, participants read a description of the stimulus and their task before completing two practice trials. The instructions indicated that particles would be moving during each trial and would appear to form an ambiguously rotating orb. An example of this stimulus was presented alongside the spinning-dancer illusion (an ambiguous motion illusion where a rotating silhouette can be perceived spinning clockwise or counterclockwise) as an example of ambiguous motion. Participants were asked to indicate the perceived direction of rotation for the orb on each trial. Following this, two practice trials were presented where a solid 3D arrow travelled around the equator of a 1000-particle orb. Each practice trial instructed participants that if the orb appears to follow the arrow, they perceive the orb travelling to the right or left, where each trial, respectively, showed the arrow travelling either rightward or leftward in front of the orb. To move to the next screen, participants had to press the arrow key (right or left) that corresponds to the direction of the arrow (see Online Resource 2 for a demonstration of these practice trials). The arrow was only

Table 1 Conditions presented within the experiment

Condition	Particle count				Cube presence		Motion congruency	
Level	1 Particle	10 Particles	100 Particles	1000 Particles	Cube absent	Cube present	Congruent motion	Incongruent motion
Details	Orb consists of 1 particle	Orb consists of 10 particles	Orb consists of 100 particles	Orb consists of 1,000 particles	Orb presented without cube	Orb presented with cube	Orb and Cube rotate the same direction	Orb and Cube rotate in opposite directions
Phase 1	1	10	100	1000				
Phase 2	1	10	100	1000	Oa	Oc	C	I

present during the practice trials to ensure that participants understood the corresponding response keys for left vs. right motion. Phase one consisted of 8 unique trials (2 orb directions X 4 particle counts) presented in random order within a block of trials. There were four blocks—and a total of 32 trials.

Phase two instructions were presented after the conclusion of phase one trials (see Online Resource 3). Instructions reiterated that the participant would observe the spinning orb again and would indicate the direction they perceived it to spin with left or right arrow key. These instructions also indicate that if participants perceive the orb's direction to change at any point, they are to indicate the new direction of motion using the left or right arrow key. There was no mention of the cube that would appear during some trials, although a cube was present with an orb on the instruction screen to demonstrate what they would view in phase two trials (for a demonstration of the instruction screen, see Online Resource 3). On half of the cube-present trials, we included a "flip" condition. On these trials, after a response was made (initial response) the cube would change direction after an average of 1.25 s (jittered from 1 to 1.5 s). Any response made after the direction change was coded as a flip response. Regardless of whether the cube changed direction, the display remained onscreen for 2 s after the initial response. Phase two consisted of 32 cube-present trials (2 orb directions X 4 particle counts X 2 initial cube directions X 2 cube flip/no-flip) with 8 cube-absent trials (2 orb directions X 4 particle counts) to make 40 trials randomized within a block. There were five blocks—each independently randomizing trial orders—for a total of 200 trials.

Results—Phase 1

Approach

A measure of response accuracy was calculated for each trial, based on the participant's response Perceived Direction of orb rotation either matching (correct) or not matching (incorrect) the Coded Direction of orb rotation. The response accuracy data were submitted to a 2 (orb Coded Direction: left or right) X 4 (particle count: **1**, **10**, **100**, **1000**) repeated-measures analysis of variance (ANOVA). Mauchly's Test of Sphericity revealed the assumption of sphericity was violated for the main effect of particle count ($W(5) = 0.48$, $p < 0.001$) and the interaction effect of orb Coded Direction and particle count ($W(5) = 0.74$, $p < 0.041$). A Greenhouse–Geisser correction was applied to the main effect of particle count ($\varepsilon = 0.68$) and the interaction effect ($\varepsilon = 0.84$). The main effect of orb Coded Direction did not approach significance ($F(1, 120) = 1.06$, $p = 0.310$), nor did its interaction with particle count ($F(2.70, 108.01) = 1.16$, $p = 0.327$). Therefore, to simplify analyses, response accuracy was collapsed across levels of orb Coded Direction and submitted to subsequent *t* tests. One sampled *t* tests were performed to compare accuracy for Coded Direction of orb rotation versus chance (defined as 50% correct responses) at each level of particle count. Then, paired samples *t* tests compared accuracy between all levels of particle count. Means and standard deviations for accuracy can be found in Table 2.

Analyses

The results of Phase 1 analyses are summarized in Fig. 3. One sample t tests compared mean response accuracy—percent of responses correctly identifying the orb's Coded Direction—against chance—50%—separately for each level of particle count. The results indicate that accuracy was significantly greater than chance for **10** ($p < 0.001$), **100** ($p < 0.001$) and **1000** ($p < 0.001$) while **1** was not significantly different from chance ($p = 0.313$). This suggests participants could identify the orb's Coded Direction for particle counts greater than one (see Fig. 3).

Paired samples *t* tests were then used to compare differential accuracy between particle counts. These tests revealed that accuracy for **1000** was significantly greater than **100** ($p < 0.001$), **10** ($p < 0.001$) and **1** ($p < 0.001$). Furthermore, **100** had better accuracy than **10** ($p < 0.001$) and **1** ($p = 0.001$). Finally, no statistical difference was observed between **10** and **1** ($p = 0.061$). This finding is consistent with the support ratio literature in that an accurate perception of

Table 2 Mean (M) and standard deviation (SD), results of one sample *t* test and the results of the paired samples *t* test

Particle count	Response accuracy (%)	One sample *t* test against 50%				Paired samples *t* test											
						1				10				100			
	M (SD)	*t*	*df*	*p* value	Cohen's *d*	*t*	*df*	*p* value	Cohen's *d*	*t*	*df*	*p* value	Cohen's *d*	*t*	df	*p* value	Cohen's d
1	53.0% (19.1%)	1.02	40	0.313	0.159												
10	60.7% (14.4%)	4.74	40	< 0.001	0.741	1.93	40	0.061	0.30								
100	69.8% (18.3%)	6.93	40	< 0.001	1.082	3.54	40	0.001	0.55	3.65	40	< 0.001	0.57				
1000	87.8% (17.3%)	13.96	40	< 0.001	2.18	8.51	40	< 0.001	1.33	9.08	40	< 0.001	1.42	6.77	40	< 0.001	1.06

Means calculated for percent response accuracy to the orb's Coded Direction in Phase 1 of the experiment (after collapsing across orb rotation directions). Results of one sample *t* test compared means against 50% response accuracy. The results of the paired samples *t* test comparing means of each combination of particle count

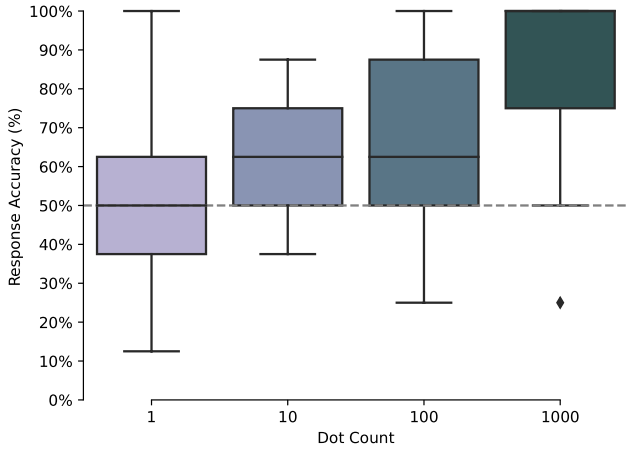

Fig. 3 Box plots of median percent response accuracy to the orb's Coded Direction from Phase 1 for each level of particle count. Lines in boxes represent median value across participants, while whiskers display 95% confidence intervals. The diamond represents outlier values (beyond 95% confidence interval). Accuracy increases from chance level (indicated by the dashed line at 50%) with increases in particle counts above one

orb direction depends upon the amount of visual information creating the percept. With more particles, the ratio of defined surface area to total surface area increased, leading to more accurate perception of the orb and its motion.

Results and discussion—Phase 2

Approach

Due to interleaving trials with and without a cube present, as well as trials where the cube changed direction, three separate analyses were conducted on Phase 2 data: response accuracy for **Oa** trials, initial response accuracy to the orb's Coded Direction for all **Oc** trials and secondary response accuracy to the orb's Coded Direction for **Oc** trials with a direction flip. The initial response **Oc** trials were first tested without considering motion congruency between the orb and cube. Next, the initial response and secondary response **Oc** trials (where the cube is present) further tested responses split by motion congruency between the orb and cube to address the impact of the cube's motion on the orb's Perceived Direction.

Orb alone

Similar to Phase 1's analysis, **Oa** responses were analyzed with one-sample *t* tests (comparing each particle count response average against chance accuracy) and paired samples *t* tests (comparing average accuracy between particle counts) to determine whether participants' percepts in Phase 2 were consistent with Phase 1. The results of the **Oa** trial's

analysis are summarized in Table 3 and Fig. 4. In comparing response accuracy against chance (50%), one sample *t* tests for each level of particle count revealed that accuracy was significantly greater than chance for **1000** ($p < 0.001$), **100** ($p < 0.001$), **10** ($p < 0.001$) and **1** ($p = 0.008$). This suggests participants could identify the orb's Coded Direction for all particle counts when the orb was presented alone.

A paired samples *t* test was used to compare response accuracy between each particle count. The pattern of results matched Phase 1's findings, showing that accuracy for **1000** was again significantly greater than **100** ($p < 0.001$), **10** ($p < 0.001$) and **1** ($p < 0.001$). Also, **100** exhibited higher accuracy than **10** ($p < 0.001$) and **1** ($p = 0.008$). Finally, no statistical difference was present between **10** and **1** ($p = 0.295$). This suggests that orb alone displays elicit similar percepts to Phase 1 even when **Oa** trials were interleaved with **Oc** trials.

Cube trials' initial responses

Means and standard deviations for accuracy to the orb's Coded Direction, as well as results of the one-sample and paired samples *t* tests can be found in Table 4 and Fig. 5. To determine whether participants could discern the orb's Coded Direction, accuracy of initial responses was split by particle count then averaged across all **Oc** trials before analyzing with one-sample *t* tests (comparing average response accuracy for each particle count against chance accuracy). In comparing response accuracy against chance (50%), one sample *t* tests for each level of particle count revealed that accuracy was significantly greater than chance for **1000** ($p < 0.001$), **100** ($p = 0.006$) and **10** ($p = 0.036$); accuracy was not significantly different from chance for **1** ($p = 0.085$). Although there was still a difference from chance found in the 10–1000 dot orbs, these differences are very small for **10** (mean = 52%) and **100** (mean = 54%). This suggests participants could identify the orb's Coded Direction for particle counts greater than **1** when the orb was presented with the cube.

To see how particle count impacted participants' ability to discern the orb's Coded Direction, a paired samples *t* test compared the average response accuracy between particle counts. Accuracy for **1000** was again significantly greater than **100** ($p < 0.001$), **10** ($p < 0.001$) and **1** ($p < 0.001$). No statistical difference was observed for any other comparison (**100** × **10**, $p = 0.213$; **100** × **1**, $p = 0.147$; **10** × **1**, $p = 0.694$). This suggests that—under the presence of the cube—the orb's Coded Direction was apparent for **1000** relative to other particle counts, but indistinguishable between lower particle counts. These findings are notably misleading, as they do not take into account the presence of the cube and whether it's direction of motion was congruent or incongruent with the orb's Coded Direction.

Table 3 Mean (M), standard deviation (SD), one sample *t* test results and paired samples *t* test results in orb alone trials of Phase 2 (after collapsing across orb rotation directions)

Particle count	Response accuracy (%)	One sample *t* test against 50%				Paired samples *t* test											
						1				10				100			
	M (SD)	*t*	*df*	*p* value	Cohen's *d*	*t*	*df*	*p* value	Cohen's *d*	*t*	*df*	*p* value	Cohen's *d*	*t*	*df*	*p* value	Cohen's *d*
1	56.8% (15.6%)	2.81	40	0.008	0.44												
10	60.7% (17.7%)	3.89	40	< 0.001	0.61	1.06	40	0.295	0.17								
100	68.3% (15.6%)	7.49	40	< 0.001	1.17	3.20	40	0.003	0.50	2.78	40	0.008	0.43				
1000	79.3% (17.7%)	10.61	40	< 0.001	1.66	6.13	40	< 0.001	0.96	5.77	40	< 0.001	0.90	4.37	40	< 0.001	0.68

Means calculated for percent response accuracy to the orb's Coded Direction at each level of particle count. Results of one sample *t* test compared means against 50% response accuracy. Results of the paired samples *t* test comparing means of each combination of particle count

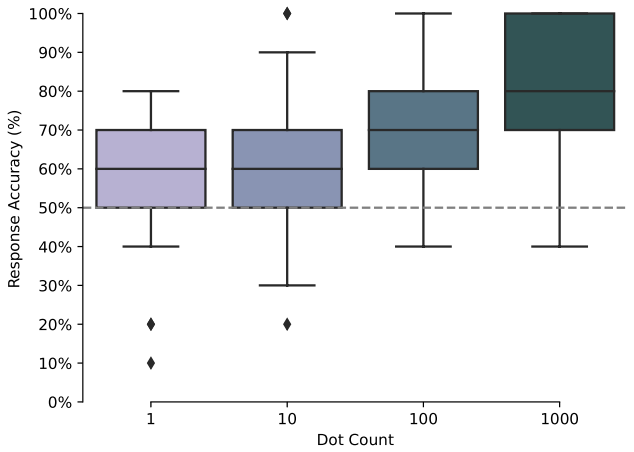

Fig. 4 Results of Phase 2's orb alone trials. Box plots show median percent response accuracy to the orb's Coded Direction for each level of particle count. Lines in boxes represent median value across participants, while whiskers display 95% confidence intervals. Diamonds represent outlier values (beyond 95% confidence interval). Similar to Phase 1 results, accuracy increases from chance level (indicated by the dashed line at 50%) with increases in particle counts. The only difference from Phase 1 is accuracy for 1 particle orbs, which are significantly greater than chance in Phase 2

To examine the impact of the cube on the orb's Perceived Direction, all **Oc** trials' initial responses to the orb's Coded Direction were entered into a 2 (motion congruence: **C** or **I**) X 4 (particle count: **1**, **10**, **100**, **1000**) ANOVA model. Means and standard deviations for accuracy to the orb's Coded Direction—split by motion congruency—can be found on Table 5. The results of the analyses can be found in Tables 5, 6, Table A in the Supplementary Materials and Fig. 6. Mauchly's Test of Sphericity revealed the assumption of sphericity was violated for the main effect of particle count ($W(5) = 0.67$, $p = 0.009$) and the interaction effect of motion congruence and particle count ($W(5) = 0.39$, $p < 0.001$). A Greenhouse–Geisser correction was applied to the main effect of particle count ($\varepsilon = 0.77$) and the interaction effect ($\varepsilon = 0.65$). Corrections did not alter results, so uncorrected values are reported below (all corrected values can be found in Table 6).

An interaction was observed between motion congruency and particle count ($F(3, 120) = 8.46$, $p < 0.001$), with accuracy being greater for **OcC** trials versus **OcI** trials (see Supplementary Materials, Table A for post hoc test results). Critically, post hoc tests with Bonferroni corrections indicate that for **OcC** trials, **1OcC** elicited reduced accuracy relative to **10OcC** ($p = 0.022$), **100OcC** ($p = 0.003$) and **1000OcC** ($p = 0.003$). Comparisons between **10OcC**, **100OcC** and **1000OcC** showed no significant differences (all p's = 1). For **OcI** trials, **1000OcI** had significantly greater accuracy as compared to **100OcI** ($p < 0.001$) and **10OcI** ($p < 0.001$), but no significant difference from **1OcI** ($p = 0.329$). **100OcI**

Table 4 Mean (M), standard deviation (SD), one sample *t* test results and paired samples *t* test results in orb alone trials of Phase 2 (after collapsing across orb rotation directions)

Particle count	Response accuracy (%)	One sample *t* test against 50%				Paired samples *t* test											
						1				10				100			
	M (SD)	*t*	*df*	*p* value	Cohen's *d*	*t*	*df*	*p* value	Cohen's *d*	*t*	*df*	*p* value	Cohen's *d*	*t*	*df*	*p* value	Cohen's *d*
1	51.8% (6.6%)	1.76	40	0.085	7.81												
10	52.3% (6.7%)	2.17	40	0.036	7.85	0.40	40	0.694	0.06								
100	53.6% (7.9%)	2.91	40	0.006	6.76	1.48	40	0.147	0.23	1.27	40	0.213	0.20				
1000	59.1% (12.8%)	4.58	40	< 0.001	4.62	4.31	40	< 0.001	0.67	4.59	40	< 0.001	0.72	4.25	40	< 0.001	0.66

Means calculated for percent response accuracy to the orb's Coded Direction at each level of particle count. The results of one sample *t* test compared means against 50% response accuracy. The results of the paired samples *t* test comparing means of each combination of particle count

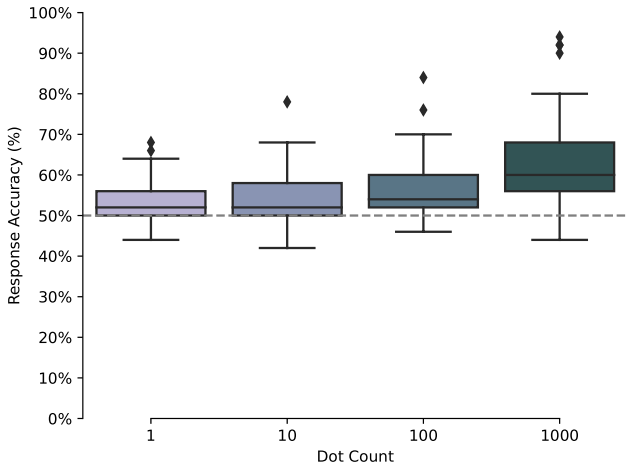

Fig. 5 Results of initial response accuracy for the orb's Coded Direction in Phase 2's orb and cube trials (after collapsing across orb and cube rotation directions). Box plots show median percent response accuracy to the orb's Coded Direction for each level of particle count. Lines in boxes represent median value across participants, while whiskers display 95% confidence intervals. Diamonds represent outlier values (beyond 95% confidence interval). Similar to Phase 1 and Phase 2 results for orb alone trials, accuracy increases from chance level (indicated by the dashed line at 50%) with increases in particle counts. In contrast to Phase 2's orb alone trials—but matching Phase 1 trials—accuracy for 1 particle orbs are not significantly greater than chance. Unlike Phase 1 and Phase 2 orb alone trials, the only significant difference in accuracy between particle counts occurred in comparisons between the 1000 particle orbs and 100, 10 and 1 particle orbs

exhibited no significant difference from **10OcI** ($p = 1$) or **1OcI** ($p = 0.510$) and **10OcI** was not significantly different from **1I** ($p = 0.077$). These findings suggest that **1000OcI** is less susceptible to motion binding than **100OcI** and **10OcI** and **1OcC** is less susceptible to motion binding as compared to all other **OcC** trial particle counts.

A main effect was observed for particle count (F (3, 120) = 12.99, $p < 0.001$) indicating differences exist in accuracy between some or all particle counts. Post hoc tests using Bonferroni corrections show that—unlike the orb alone analysis—a significant increase in accuracy was only observed for **1000Oc** ($p < 0.001$), although these findings are misleading in light of the interaction which showed that accuracy is highly dependent on motion congruency. There was also a main effect for motion congruency (F (1, 40) = 121.24, $p < 0.001$) such that **OcC** trials had greater accuracy as compared to **OcI** trials. This suggests the cube interfered with participants' perception of the orb's direction.

Cube trials' secondary responses

Oc trials' secondary responses when a direction flip occurred were entered into a 2 (motion congruence: **C** or **I**) X 4 (particle count: **1**, **10**, **100**, **1000**) ANOVA model. Analysis results can be found in Tables 7, 8, Table B in the Supplementary Materials and Fig. 7. Mauchly's Test of Sphericity revealed the assumption of sphericity was violated for the interaction effect of motion congruence and particle count (W (5) = 0.35, $p < 0.001$). A Greenhouse–Geisser correction was applied to the interaction effect ($\varepsilon = 0.59$). Similar to the initial response analysis, there was an interaction of motion congruency and particle count (F (3, 120) = 3.59, $p = 0.016$), with greater accuracy for **OcC** trials versus **OcI** trials (see Supplementary Materials, Table B for post hoc test results). Critically, post hoc tests with Bonferroni corrections indicate **1000OcC** trials showed greater accuracy than **1OcC** ($p = 0.006$), but no significant difference from **100** and **10OcC** ($p = 1$). **100OcC** showed a significant difference from **1OcC** ($p = 0.017$), but no significant difference from **10OcC** ($p = 1$). **10OcC** was not significantly different from **1OcC** ($p = 0.165$). There were no significant differences between all combinations of **OcI** trials ($p = 1$). This suggests that **1OcC** is less susceptible to motion binding, even with a perceptual flip, than **1000OcC** and **100OcC**.

Table 5 Mean (M), standard deviation (SD) and one sample t test results for initial response accuracy to the orb's Coded Direction in orb and cube trials of Phase 2 (after collapsing across orb rotation directions)

Orb and Cube motion congruency	Particle count	Response accuracy (%)	One sample t test against 50%			
		M (SD)	t	df	p value	Cohen's d
Congruent	1	83% (22%)	9.66	40	< 0.001	1.51
	10	91% (20%)	13.25	40	< 0.001	2.07
	100	92% (21%)	12.81	40	< 0.001	2.00
	1000	92% (19%)	14.01	40	< 0.001	2.19
Incongruent	1	21% (24%)	− 7.83	40	< 0.001	− 1.22
	10	14% (22%)	− 10.49	40	< 0.001	− 1.64
	100	15% (26%)	− 8.67	40	< 0.001	− 1.35
	1000	26% (32%)	− 4.83	40	< 0.001	− 0.75

Means calculated for percent response accuracy to the orb's Coded Direction at each level of particle count for trials where the orb and cube motion direction is congruent or incongruent. Results of one sample t test compared means against 50% response accuracy

Table 6 ANOVA results for initial response accuracy to the orb's Coded Direction in orb and cube trials of Phase 2 (after collapsing across orb rotation directions)

Predictor	SS_{Num}	SS_{Den}	Epsilon	df_{Num}	df_{Den}	MSE	F	p	η_p^2
Motion congruency	40.95	13.51		1	40	0.34	121.24	< 0.001	0.75
Particle count	0.28 (0.28)	0.86	0.77	3 (2.32)	120 (92.76)	0.01 (0.01)	12.99 (12.99)	< 0.001 (< 0.001)	0.25 (0.25)
Particle count * Motion congruency	0.35 (0.35)	1.64	0.65	3 (1.96)	120 (78.31)	0.01 (0.02)	8.46 (8.46)	< 0.001 (< 0.001)	0.17 (0.17)

Note. df_{Num} indicates degrees of freedom numerator. df_{Den} indicates degrees of freedom denominator. Epsilon indicates Greenhouse–Geisser multiplier for degrees of freedom, Mean Square Error (*MSE*) and p values in the table incorporate this correction. SS_{Num} indicates the sum of squares numerator. SS_{Den} indicates the sum of squares denominator. η_p^2 indicates partial eta-squared

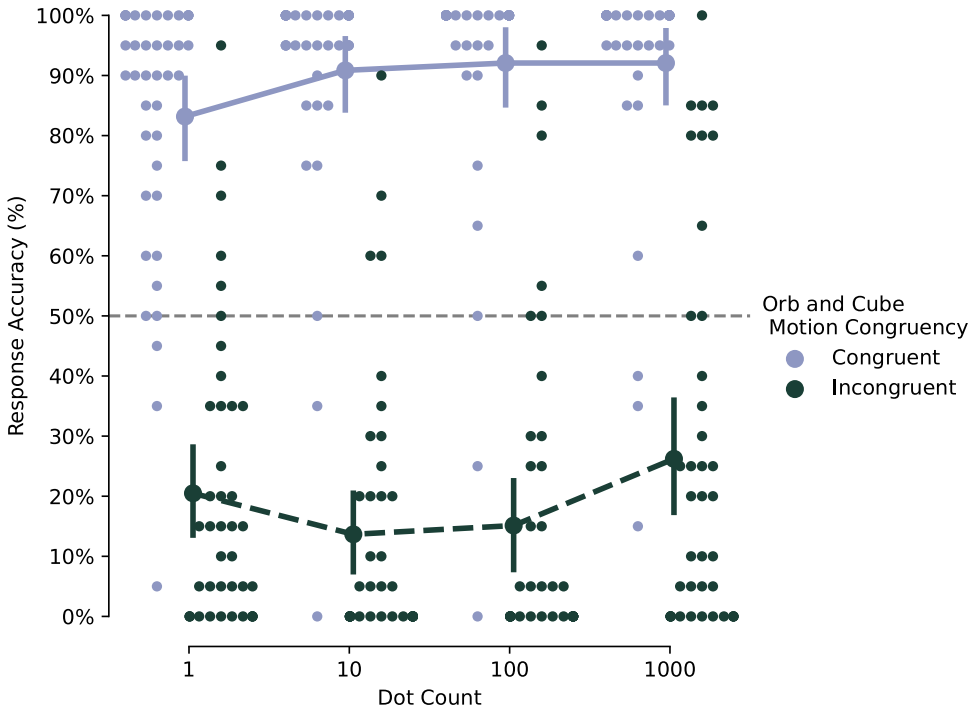

Fig. 6 Results of initial response accuracy for the orb's Coded Direction when congruent versus incongruent with the cube's direction in orb and cube trials of Phase 2 (after collapsing across orb rotation directions). Plotted are each participant's mean response (unconnected dots) and means of all participants (connected dots) for each level of particle count. Whiskers represent 95% confidence intervals

Table 7 Mean (M), standard deviation (SD) and one sample *t* test results for secondary response accuracy to the orb's Coded Direction in orb and cube trials of Phase 2 (after collapsing across orb rotation directions)

Orb and cube motion congruency	Particle count	Response accuracy (%)	One sample *t* test against 50%			
		M (SD)	*t*	*df*	*p* value	Cohen's *d*
Congruent	1	67% (28%)	3.83	40	< 0.001	0.60
	10	75% (27%)	5.99	40	< 0.001	0.94
	100	78% (30%)	5.95	40	< 0.001	0.93
	1000	79% (24%)	7.60	40	< 0.001	1.19
Incongruent	1	34% (28%)	− 3.54	40	0.001	− 0.55
	10	29% (31%)	− 4.33	40	< 0.001	− 0.68
	100	30% (33%)	− 3.75	40	< 0.001	− 0.59
	1000	34% (35%)	− 2.96	40	0.005	− 0.46

Means calculated for percent response accuracy to the orb's Coded Direction at each level of particle count for trials where the orb and cube motion direction is congruent or incongruent. Results of one sample *t* test compared means against 50% response accuracy

Table 8 ANOVA results for secondary response accuracy to the orb's Coded Direction in orb and cube trials of Phase 2 (after collapsing across orb rotation directions)

Predictor	SS_{Num}	SS_{Den}	Epsilon	df_{Num}	df_{Den}	MSE	F	p	η_p^2
Motion congruency	14.85	22.02		1	40	0.55	26.99	< 0.001	0.35
Particle count	0.15	1.56		3	120	0.01	3.82	0.012	< 0.01
Particle count * Motion Congruency	0.30 (0.30)	3.34 (3.34)	0.59	3 (1.77)	120 (70.64)	0.03 (0.05)	3.59 (3.59)	0.016 (0.038)	0.01 (0.01)

Note. df_{Num} indicates degrees of freedom numerator. df_{Den} indicates degrees of freedom denominator. *Epsilon* indicates Greenhouse–Geisser multiplier for degrees of freedom, Mean Square Error (MSE) and p values in the table incorporate this correction. SS_{Num} indicates the sum of squares numerator. SS_{Den} indicates the sum of squares denominator. η_p^2 indicates partial eta-squared

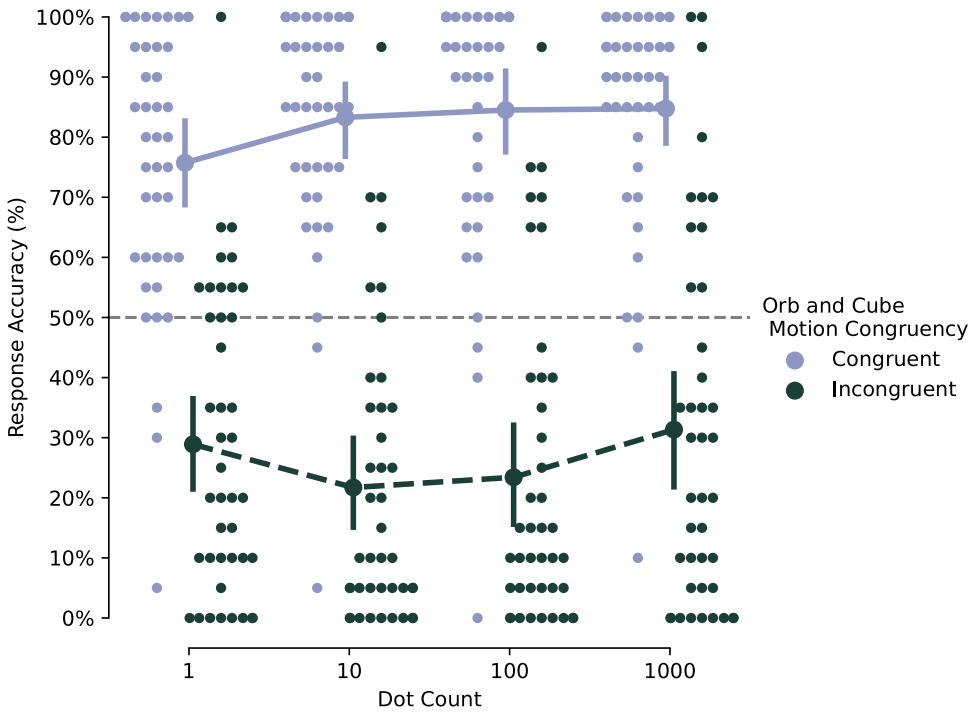

Fig. 7 Results from Phase 2 flip direction analysis. Plots show all responses (unconnected dots) and means (connected dots) for each level of particle count. The whiskers represent 95% confidence intervals. The plot shows percent response accuracy for the orb's Coded Direction when congruent versus incongruent with the cube's direction

There was a main effect of motion congruency (F (1, 40) = 26.99, $p < 0.001$), with congruency leading to greater accuracy, suggesting that even after the cube direction flips, the cube continued to interfere with participants' perception of the orb's motion. There was also a main effect of particle count (F (3, 120) = 3.82, $p = 0.012$). Post hoc tests with Bonferroni corrections indicate that accuracy was greater for **1000Oc** as compared to **1Oc** (t (40) = 3.22, $p = 0.010$), but no other significant differences were observed between the comparisons for **1000Oc** and **100Oc** ($p = 1$), **1000Oc** and **10Oc** ($p = 0.154$), **100Oc** and **10Oc** ($p = 1$), **100Oc** and **1Oc** ($p = 0.296$) and **10Oc** and **1Oc** ($p = 1$). These findings are misleading given the results of the interaction which showed that accuracy is highly dependent on motion congruency being either **OcC** or **OcI**.

As would be expected, an increase in particle count led to an increase in accuracy for Coded Direction on trials only presenting the orb (see Fig. 3). This was the case even when **Oa** trials were shuffled with **Oc** trials during Phase 2 (see Fig. 4). When observing **Oc** trials, accuracy for Coded Direction appears to suffer for all particle counts when not considering the cube (see Fig. 5). This is a misleading conclusion, as Perceived Motion clearly binds to the cube's direction when considering motion congruency between orb and cube (see Fig. 6). For **OcI** trials, the cube appears to dominate Perceived Motion at **10OcI** and **100OcI** particles, while this interference weakens for **1000OcI** trials as seen by the increased mean accuracy (see Fig. 6). This observation is further highlighted by the responses for motion direction congruency. Even when the cube direction flips, participants were more likely to update their percept of the orb's

direction to match (see Fig. 7). Altogether, this suggests that motion perception is being strongly influenced by the cube.

Although global motion perception appears to be bound to the cube, there is a subtle connection between the particle count and strength of the cube's interference. For **1OcC** and **1OcI** trials, participants were less likely to indicate the orb as moving the same direction as the cube regardless of their actual motion congruency. Similarly, participants were less prone to perceiving congruent motion for **OcI** trials. These findings suggest that there is an ideal stimulus complexity which reliably leads to the illusion's motion binding.

General discussion

The present study found the Z-Box Illusion to be a novel perceptual illusion wherein an unambiguous, task-irrelevant contextual stimulus influences perception of an ambiguous motion stimulus. When viewing an orb alone, participants were able to determine the orb's Coded Direction. In contrast, when participants observed the orb with an unambiguous, task-irrelevant contextual stimulus—the cube—their responses suggest the orbs' direction strongly influences the cube's perceived direction. Although perception of the orb's motion was strongly influenced by the cube at all particle counts, it is important to note that participants did not simply report the direction of the cube on every trial (see Fig. 6 for variance in participant's responses to congruent and incongruent trials). This suggests that participants were trying to determine the actual motion of the cube rather than just defaulting to the more stable structure of the cube. Variations in the orb's particle count contribute to this effect in two ways. When a single particle rotates in isolation, viewers are unable to determine the orb's Coded Direction in Phase 1. This leads to less motion conflation when viewing the orb and cube together. In contrast, 1000 particles led to the most accurate detection of Coded Direction for the orb alone. This also reduced motion conflation between the orb and cube. Unexpectedly, the single particle orb had greater than chance accuracy in Phase 2. This could potentially be the result of practice and prolonged exposure to similar perceptual cues for the more complex orb structures (particle location, trajectory, speed of motion). These findings elucidate the foundations for this novel illusion.

The results suggest that participants could determine the Coded Direction of the orb and this observation is linked to the orb's particle count. Previously, the particle orb was believed to be a bistable percept. The finding that participants could determine the orb's Coded Direction is supported by studies examining SFMs relationship to rigid-body objects (objects defined by elements rotating about a fixed axis). Originally, Ullman (1979) determined—through a mathematical theorem—how SFM object direction can be extrapolated accurately with at least four defining points. Ullman (1984) later updated his theory, showing that accuracy increases with viewing time and particle count. Similarly, Hoffman and Bennett (1986) found that two points are sufficient to generate a stable percept if rotational speed is assumed to be constant while three defining points generate a bistable percept. Unfortunately, none of these studies touch on prior experience as a potential contribution to direction determination. Prior experience or practice seem to improve direction identification in ambiguous stimuli, as observed in the difference between the single particle orb of Phase 1 and the single particle orb (orb alone trials) of Phase 2. Regardless, these studies help explain most differences observed between particle counts.

Beyond simple observations of the orb, the results from phase two—orb and cube presentations—expand upon findings from studies of ambiguous stimuli. In the study of feature-based attention (Yu et al., 2017), the features of task-irrelevant stimuli have been found to bias perceptions of task-relevant stimuli. This is particularly relevant given the stimuli presented were also ambiguous, particle-based SFM structures. This would suggest that a stable object such as the cube is unnecessary and could be replaced with ambiguous SFM structures similar to the orb. Future studies could examine the secondary object's stability in relationship to the illusion to determine if there are any unique contributions based on ambiguity or object shape. Although it is uncertain how critical stability is to the illusion, the present study extends the findings of Yu et al. (2017) to include structural integrity (i.e. the cubes' stable percept versus the orb's potential bistability) as a feature which influences task-relevant perception.

The significance of structural integrity and motion perception similarly relate to the motion aperture problem. The ambiguity of local motion information (i.e. the 10 and 100 particle orbs) seems to resolve when less ambiguous stimuli are present (i.e. the edge-defined cube). As more particles are present in the 1000 particle orb, perception of the orb's Coded Direction begins to return. The approach towards baseline motion perception appears similarly to the opening of the aperture around local motion, revealing the true nature of the stimuli underneath.

One alternative explanation for the binding of the orb and cube may be due to common fate. Although initially thinking that the orb and cube would be viewed as distinct and separate objects, the similar size and rotational velocity of the orb and cube suggest that these items could be seen as a single item. This inference would reinforce the expectation that these items were moving the same direction. Although this manipulation was not in the present study, it would be valuable to determine what role common fate plays in the orb's Perceived Direction when viewed with the cube.

Finally, the present study highlights the perception of SFM while extending this work with feature integration. The findings suggest ways to manipulate or improve motion perception for 3D stimuli. First, structural integrity appears to dominate motion perception. Further, the motion of ambiguous objects can be heavily influenced by a stable objects' motion. Taken together, strong—yet irrelevant—objects could be utilized to better manage scenarios where ambiguous motion perception in objects is critical.

Supplementary Information The online version contains supplementary material available at https://doi.org/10.1007/s00426-021-01589-0.

Acknowledgements This project was supported by National Science Foundation OIA 1632849 to MDD and colleagues. The authors would like to thank our research assistant Joshua Warren, who provided invaluable assistance in data collection and presentation of findings.

Author contributions Both authors contributed to the study conception and design. Material preparation, data collection and analysis were performed by JEZ. The first draft of the manuscript was written by JEZ and both authors commented on previous versions of the manuscript. Both authors read and approved the final manuscript.

Funding This project was supported by NSF OIA 1632849 (RII Track-2 FEC: Neural networks underlying the integration of knowledge and perception) to MDD and colleagues.

Availability of data and material The datasets generated during and/or analyzed during the current study are available from the corresponding author upon request.

Code availability Experimental and data processing code are available from the corresponding author upon request.

Declarations

Conflict of interest The authors have no relevant financial or non-financial interests to disclose.

Ethics approval The approval was obtained from the ethics committee of University of Nebraska – Lincoln. The procedures used in this study adhere to the tenets of the Declaration of Helsinki.

Consent to participate Informed consent was obtained from all individual participants included in the study.

Consent for publication Participants signed informed consent regarding publishing their anonymous data.

References

Andersen, R. A., & Bradley, D. C. (1998). Perception of three-dimensional structure from motion. *Trends in Cognitive Sciences, 2*(6), 222–228. https://doi.org/10.1016/S1364-6613(98)01181-4

Bradley, D. R., & Petry, H. M. (1977). Organizational determinants of subjective contour: The subjective necker cube. *The American Journal of Psychology, 90*(2), 253–262. https://doi.org/10.2307/1422047 JSTOR.

Caudek, C., & Domini, F. (1998). Perceived orientation of axis rotation in structure-from-motion. *Journal of Experimental Psychology: Human Perception and Performance, 24*(2), 609.

Domini, F., & Caudek, C. (2003). 3-D structure perceived from dynamic information: A new theory. *Trends in Cognitive Sciences, 7*(10), 444–449.

Domini, F., & Caudek, C. (2010). Matching perceived depth from disparity and from velocity: Modeling and psychophysics. *Acta Psychologica, 133*(1), 81–89.

Domini, F., Vuong, Q. C., & Caudek, C. (2002). Temporal integration in structure from motion. *Journal of Experimental Psychology: Human Perception and Performance, 28*(4), 816.

Erlikhman, G., Caplovitz, G. P., Gurariy, G., Medina, J., & Snow, J. C. (2018). Towards a unified perspective of object shape and motion processing in human dorsal cortex. *Consciousness and Cognition, 64*, 106–120. https://doi.org/10.1016/j.concog.2018.04.016

Erlikhman, G., Fu, M., Dodd, M. D., & Caplovitz, G. P. (2019). The motion-induced contour revisited: Observations on 3-D structure and illusory contour formation in moving stimuli. *Journal of Vision, 19*(1), 7–7. https://doi.org/10.1167/19.1.7

Faul, F., Erdfelder, E., Lang, A. G., & Buchner, A. (2007). G* Power 3: A flexible statistical power analysis program for the social, behavioral, and biomedical sciences. *Behavior Research Methods, 39*(2), 175–191. https://doi.org/10.3758/BF03193146

Hoffman, D. D., & Bennett, B. M. (1986). The computation of structure from fixed-axis motion: Rigid structures. *Biological Cybernetics, 54*(2), 71–83. https://doi.org/10.1007/BF00320477

Jain, A., & Zaidi, Q. (2011). Discerning nonrigid 3D shapes from motion cues. *Proceedings of the National Academy of Sciences, 108*(4), 1663–1668.

Köhler, W. (1970). *Gestalt psychology: An introduction to new concepts in modern psychology* (Vol. 18). WW Norton & Company.

Miles, W. R. (1931). Movement interpretations of the Silhouette of a Revolving Fan. *The American Journal of Psychology, 43*(3), 392–405. https://doi.org/10.2307/1414610 JSTOR.

Nawrot, M., & Blake, R. (1989). Neural integration of information specifying structure from stereopsis and motion. *Science, 244*(4905), 716. https://doi.org/10.1126/science.2717948

Ramachandran, V. S., Cobb, S., & Rogers-Ramachandran, D. (1988). Perception of 3-D structure from motion: The role of velocity gradients and segmentation boundaries. *Perception & Psychophysics, 44*(4), 390–393. https://doi.org/10.3758/BF03210423

Rogers, B., & Graham, M. (1979). Motion parallax as an independent cue for depth perception. *Perception, 8*(2), 125–134.

Shipley, T. F., & Kellman, P. J. (1992). Strength of visual interpolation depends on the ratio of physically specified to total edge length. *Perception & Psychophysics, 52*(1), 97–106. https://doi.org/10.3758/BF03206762

Treue, S., Husain, M., & Andersen, R. A. (1991). Human perception of structure from motion. *Vision Research, 31*(1), 59–75. https://doi.org/10.1016/0042-6989(91)90074-F

Ullman, S. (1979). The interpretation of structure from motion. *Proceedings of the Royal Society of London. Series b. Biological Sciences, 203*(1153), 405–426.

Ullman, S. (1984). Maximizing rigidity: The incremental recovery of 3-D structure from rigid and Nonrigid motion. *Perception, 13*(3), 255–274. https://doi.org/10.1068/p130255

Wallach, H., & O'Connell, D. N. (1953). The kinetic depth effect. *Journal of Experimental Psychology, 45*(4), 205–217. https://doi.org/10.1037/h0056880

Weiss, Y., & Adelson, E. H. (1998). Slow and smooth: A Bayesian theory for the combination of local motion signals in human vision. Technical report A.I. Memo No. 1624, MIT.

Weiss, Y., & Adelson, E. H. (2000). Adventures with gelatinous ellipses—constraints on models of human motion analysis. *Perception, 29*(5), 543–566.

Weiss, Y., Simoncelli, E. P., & Adelson, E. H. (2002). Motion illusions as optimal percepts. *Nature Neuroscience, 5*(6), 598–604.

Wuerger, S., Shapley, R., & Rubin, N. (1996). "On the visually perceived direction of motion" by Hans Wallach: 60 years later. *Perception, 25*(11), 1317–1367. https://doi.org/10.1068/p251317

Yu, D., Levinthal, B., & Franconeri, S. L. (2017). Feature-based attention resolves depth ambiguity. *Psychonomic Bulletin & Review, 24*(3), 804–809. https://doi.org/10.3758/s13423-016-1155-x